CONF-891007--44

by OSTI

NOV 0 6 1989

UCRL--101063

DE90 002234

A 14-MeV Beam-Plasma Neutron Source for Materials Testing

A.H. Futch
F.H. Coensgen
C.C. Damm
A.W. Molvik

This paper was prepared for submittal to
13th Symposium on Fusion Engineering
Knoxville, TN, October 2–6, 1989

Lawrence Livermore National Laboratory

This is a preprint of a paper intended for publication in a journal or proceedings. Since changes may be made before publication, this preprint is made available with the understanding that it will not be cited or reproduced without the permission of the author.

DISCLAIMER

This report was prepared as an account of work sponsored by an agency of the United States Government. Neither the United States Government nor any agency thereof, nor any of their employees, makes any warranty, express or implied, or assumes any legal liability or responsibility for the accuracy, completeness, or usefulness of any information, apparatus, product, or process disclosed, or represents that its use would not infringe privately owned rights. Reference herein to any specific commercial product, process, or service by trade name, trademark, manufacturer, or otherwise does not necessarily constitute or imply its endorsement, recommendation, or favoring by the United States Government or any agency thereof. The views and opinions of authors expressed herein do not necessarily state or reflect those of the United States Government or any agency thereof.

MASTER

DISTRIBUTION OF THIS DOCUMENT IS UNLIMITED

DISCLAIMER

This document was prepared as an account of work sponsored by an agency of the United States Government. Neither the United States Government nor the University of California nor any of their employees, makes any warranty, express or implied, or assumes any legal liability or responsibility for the accuracy, completeness, or usefulness of any information, apparatus, product, or process disclosed, or represents that its use would not infringe privately owned rights. Reference herein to any specific commercial products, process, or service by trade name, trademark, manufacturer, or otherwise, does not necessarily constitute or imply its endorsement, recommendation, or favoring by the United States Government or the University of California. The views and opinions of authors expressed herein do not necessarily state or reflect those of the United States Government or the University of California, and shall not be used for advertising or product endorsement purposes.

A 14-MEV BEAM-PLASMA NEUTRON SOURCE FOR MATERIALS TESTING

A.H. Futch, F.H. Coensgen, C.C. Damm, and A.W. Molvik
Lawrence Livermore National Laboratory
P.O. Box 5511, L-637
Livermore, CA 94551

ABSTRACT. The design and performance of 14-MeV beam-plasma neutron sources for accelerated testing of fusion reactor materials are described. Continuous production of 14-MeV neutron fluxes in the range of 5 to 10 MW/m^2 at the plasma surface are produced by D-T reactions in a two-component plasma. In the present designs, 14-MeV neutrons result from collisions of energetic deuterium ions created by transverse injection of 150-keV deuterium atoms on a fully ionized tritium target plasma. The beam energy, which is deposited at the center of the tritium column, is transferred to the warm plasma by electron drag, which flows axially to the end regions. Neutral gas at high pressure absorbs the energy in the tritium plasma and transfers the heat to the walls of the vacuum vessel. The plasma parameters of the neutron source, in dimensionless units, have been achieved in the 2XIIB high-β plasma. The larger magnetic field of the present design permits scaling to the higher energy and density of the neutron source design. In the extrapolation, care has been taken to preserve the scaling and plasma attributes that contributed to equilibrium, magnetohydrodynamic (MHD) stability, and microstability in 2XIIB. The performance and scaling characteristics are described for several designs chosen to enhance the thermal isolation of the two-component plasmas.

I. Introduction

In this paper we describe several designs for a 14-MeV neutron source based on the deuterium-tritium (D-T) reaction. In all present designs, the reactions proceed in a linear two-component plasma produced by transverse injection of 150-keV deuterium atoms into a fully ionized tritium target plasma. Parameters for such a neutron source are selected to meet the requirements for accelerated testing of materials in a fusion materials development program. The overall objective of such a program is to develop new or improved materials with long lives and low activation under 14-MeV neutron irradiation. A plasma-based fusion source would avoid questions of extrapolation because of differences in the neutron energy spectrum and would give valuable design information of synergistic effects in this complex environment.

For accelerated materials testing, source characteristics must be related to anticipated reactor goals. The relevant reactor goals[1] are for a minimum neutron wall loading of 3-6 MW/m^2, a minimum first-wall lifetime of 2-5 yr, and hence a *minimum integrated neutron wall loading* of ~10-20 $MW{\cdot}yr/m^2$.

In approaching a design for a compact, intense neutron source, we review linear systems based on high-density two-component plasmas. The basic plasma physics of the reaction region is based on the stable operation of the neutral-beam-driven 2XIIB experiment.[2] We first discuss the thermal isolation and power transport for the "flow" and "multiple mirror" models. Finally we focus on the high-density two-component plasma system with power losses limited by electron thermal conductivity. Our design goal for the high-fluence neutron source was chosen as an uncollided 14-MeV neutron flux equivalent to 10 MW/m^2, to provide the required radiation dose for materials testing in approximately 1–2 yr.

II. Neutron Source Concepts

In the design studies discussed here for beam-plasma neutron sources, D-T neutrons are produced by injecting a current of energetic deuterium atoms into a dense, fully ionized tritium plasma column. As an example, Fig. 1 shows a schematic diagram of the neutron source for the electron thermal conductivity case, or Spitzer model. Except for the power transport region, other beam-plasma designs are similar. As shown in Fig. 1, the high-density target plasma and the hot deuterium plasma that is formed by ionization of the transverse-injected D° current are confined by a linear array of magnets. The usually difficult problem posed by disposal of beam power deposited in the target is solved by conducting the injected power along the plasma column to large area end tanks.

The target plasma is sufficiently dense to stop most of the injected D° particles, and it is hot enough (electron temperature $T_e \simeq 0.2$ keV) to increase the D-T reaction rate significantly above that obtained with solid targets. The trapped deuterons cool to the temperature of the target plasma and eventually diffuse out the ends of the device. Energy transfer between hot deuterium ions and electrons heats the tritium ions, so the warm-ion temperature $T_i \leq T_e$ in the plasma column. Evaluations of an optimum beam energy for two-component plasmas have shown a broad maximum to exist at ~200 keV.[3] Figure 2 shows Q, the ratio of fusion power to injection power, as a function of the deuteron injection energy from the paper by Post et al.[3] For a fixed electron temperature, the maximum value of Q occurs at approximately 200 keV. Since the efficiency of positive-ion beam technology is adequate for ion energies up to 150 keV, we have chosen 150 keV as the injection energy, thus avoiding the need for an expensive and protracted development based on negative-ion beams. The reaction rate is decreased about 20% by this compr[illegible]ise.

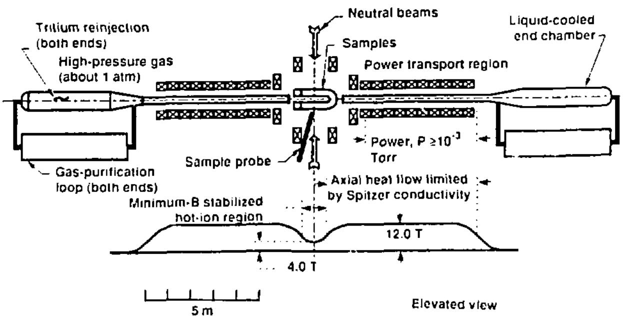

FIG. 1 Schematic of beam plasma neutron source. Central section of vacuum chamber and neutron shielding of superconducting magnets are not shown

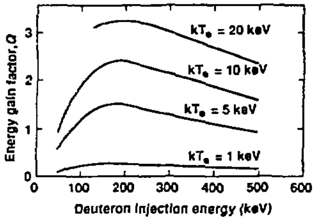

FIG. 2. Energy gain factor Q vs injection energy and electron temperature T_e for a mirror ratio $R = 10(kT_i = kT_e)$.

III. Reaction Chamber Plasma Model

Because radial density profiles in neutral-beam-driven linear systems are observed to be Gaussian, we model the plasma with a radial density of the form $n = \hat{n}e^{-(r/a)^2}$, where a is the e-folding distance for the density fall-off. To enhance the plasma density and consequently the reaction rate, we inject the neutral beam off-axis where the plasma density is $n_e = \hat{n}_e e^{-1}$. To fuel the center of the plasma and to minimize the plasma radius, we direct the neutral beam so the D^+ ions curve toward the axis, as shown in Fig. 3. The magnetic field at the injection position is chosen so $2\rho = a$, where ρ is the gyroradius of the hot deuterium ion.

The total plasma density is determined by beam penetration. As a condition for beam penetration with nearly complete beam absorption, we chose the line density to the midpoint along the chord through the plasma to be equal to $2\sigma_{trap}^{-1}$:

$$\int_{-\infty}^{a} n_e dl = \frac{2\sigma_{trap}^{-1}}{(1+\delta)}, \tag{1}$$

where σ_{trap} includes beam ionization by electrons and ions as well as charge-exchange collisions, and δ is the correction factor for multiple-collision enhancement[4] of trapping. This condition determines the total plasma density. Figure 3 shows the geometry for pencil beam injection

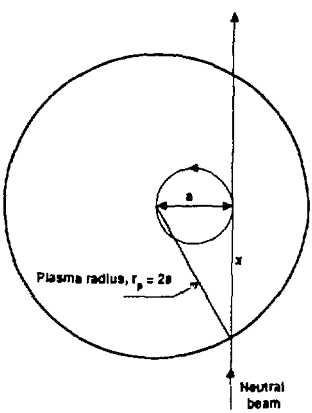

FIG. 3. Neutral beam injection geometry. Central ray of neutral beam is located one orbit diameter from axis for full energy D^+. Magnetic field direction is chosen so velocity of injected ions is toward plasma center.

along a chord where the electron density $n_e = \hat{n}_e e^{-[(a^2+x^2)/a^2]}$ and the line density is

$$\int_{-\infty}^{a} n_e dl = \hat{n}_e \frac{\sqrt{\pi}}{2} e^{-1} a = 0.326\hat{n}_e a \,. \tag{2}$$

By equating Eqs. (1) and (2), we find:

$$\hat{n}_e = \frac{2\sigma_{trap}^{-1}}{0.326a(1+\delta)} \,. \tag{3}$$

The condition for validity of the flow model is that the electron mean free path λ is greater than $l_c/2$; this requirement results in the following expression for the maximum electron density:

$$\hat{n}_e < 3.4 \times 10^{22} T_e^2 / l_c \,, \tag{4}$$

where l_c is the full length of the plasma column. The peak hot-ion density is determined from the expression for $\hat{\beta}$:

$$\hat{n}_h = \frac{\hat{\beta} B^2}{4 \times 10^{-22} E_h} \cdot \text{ions/m}^3 \,, \tag{5}$$

where E_h is the average hot-ion energy in keV (determined separately from a Fokker-Planck code) and B is the magnetic field in tesla.

IV. Thermal Isolation and Parallel Power Flow

A. Flow Model

If the electron mean free path is longer than the midplane-to-mirror distance, then mass flow dominates over electron thermal conductivity, and the heat flow per unit area, Q_f, through the magnetic mirrors is

$$Q_f = 1 \times 10^{-3} \frac{n_T v_s}{2} e \frac{\eta T_e}{R} \cdot \text{MW/m}^2 \,, \tag{6}$$

with v_s the sound speed and $\eta = \phi + T_e$ where ϕ is the plasma potential. Both ϕ and T_e are expressed in keV. With $\phi \approx 4.3T_e$, and

$$v_s = \sqrt{[T_e + (5/3)T_i]/m_h} = 1.77 \times 10^5 \rho T_e^{1/2} \cdot \text{m/s} \,, \tag{7}$$

where $\rho = [1 + 5/3(\frac{T_i}{T_e})]^{1/2}$ and m_h the triton mass, we obtain

$$Q_f = 1.42 \times 10^{-17} \rho n_T T_e^{3/2} \eta / R \cdot \text{MW/m}^2 \,. \tag{8}$$

For a cylindrical plasma of unit cross-sectional area and hot-ion length l_h, the electron drag on the hot deuterium ions is

$$Q_{drag} = \frac{n_e n_h E_h e l_h}{(n\tau_{drag})} = 9.3 \times 10^{-41} \frac{n_h n_e E_h l_h}{T_e^{\frac{3}{2}}} \cdot \text{MW/m}^2 \,, \tag{9}$$

where n_e is the total density, n_h the hot density, E_h the average hot-ion energy, e the electronic charge, and $(n\tau)_{drag} = 1 \times 10^{19} A_i T_e^{3/2} (1/\ln\Lambda)$. Therefore, for deuterons, where $\ln\Lambda = 11.6$, $(n\tau)_{drag} \doteq 1.72 \times 10^{18}\, T_e^{3/2}$ (keV).

Assuming only axial heat loss, we equate $Q_f = Q_{drag}$ on the axis and solve for $\hat{T}_e$, obtaining

$$\hat{T}_e = 1.87 \times 10^{-8} \left[\frac{n_e n_h E_h l_h R}{n_T \eta \rho}\right]^{\frac{1}{3}} \cdot \text{keV} \tag{10}$$

for the peak electron temperature. We estimate E_h from the expression $E_h = E_I / \ln(E_I/20T_e)$, where E_I is the hot deuterium injection energy.

For a Gaussian radial density profile, the axial power flow P_f becomes

$$P_f = 2\pi \left(1.42 \times 10^{-17}\right) \eta \frac{\hat{n}_T \hat{T}_e^{\frac{3}{2}}}{R} \rho \int_0^{2a} e^{-(\frac{r}{a})^2} r dr \cdot \text{MW} \tag{11}$$

where we have neglected the complex dependence of T_e with radius. For $a = .039$ m, $\eta = 5.3$, and $R = 3$,

$$P_f = 1.22 \times 10^{-19} n_T T_e^{\frac{3}{2}} \rho \cdot \text{MW} \,. \tag{12}$$

For the flow model, the confinement time for warm tritium plasma is not sufficiently long for equilibrium to be established with the electrons. We estimate the tritium-ions temperature from analytic equations to be ≈ 0.1 keV for the parameters of Table I.

As a check on the simple flow equations discussed here, we have calculated a neutron source case using the FPPAC multispecies Fokker-Planck code.[5] For this example, the midplanar magnetic field is 4 T, the magnetic mirror ratio is 3, $l_h = 0.15$ m, $l_c = 1$ m, ϕ/T_e is set equal to 4.3, $v_s = 1.35 \times 10^5$ m/s, $n_e = 2.36 \times 10^{21}$, and $n_h = 1.03 \times 10^{21}$. Table I shows a comparison between the Fokker-Planck code and the simple analytic equations. In general, the agreement is good.

Table I: Comparison of Equilibrium Plasma Parameters from Analytic Equations with Parameters from the FPPAC Fokker-Planck Code.

Parameter	Analytic Equations	FPPAC Code
n_e (electrons/m^3)^a	2.36×10^{21}	2.36×10^{21}
n_h (ions/m^3)^a	1.03×10^{21}	1.03×10^{21}
n_T (ions/m^3)^a	1.34×10^{21}	1.34×10^{21}
T_e (keV)	0.40	0.38
E_h (keV)	51.0	46
T_i (keV)	0.11	0.117
P_f (MW)	50	62
Γ (MW/m^2)^b	4.4	4.4

^{a}All densities are input parameters.
$^b\sigma v = 4.31 \times 10^{-22}$ m^3/s

B. Multiple-Mirror Model

Additional thermal isolation may be achieved by the use of multiple mirrors.[6] If the scale lengths are such that

$$l_m \ll \lambda_e \ll R l_c ,$$

where l_m is the magnetic field scale length and l_c is the mirror cell length, then the power flux for a multiple mirror is

$$Q_f = 1 \times 10^{-3} \frac{n_T v_s}{2} e\eta \frac{T_e}{R} \left[\frac{l_c}{L} K \right] , \qquad (13)$$

where L is the total system length and K is a parameter which varies between 1 and 2, approaching 2 for a large number of mirror cells.

Solving Eq. (9) for $T_e^{\frac{3}{2}}$ and substituting into the expression for Q_f gives

$$Q_f = 3.62 \times 10^{-29} \left[\frac{\eta n_h n_e n_T E_h l_h K l_c \rho}{RL} \right]^{\frac{1}{2}} \cdot \mathrm{MW/m^2} , \qquad (14)$$

with $\eta = 5.3$. Since $Q_f = Q_{drag}$, the net result is that for the same plasma parameters and wall loading, a multiple-mirror neutron source requires less input power by the factor $(K l_c/L)^{\frac{1}{2}}$.

C. Conductivity Model

For the Spitzer conductivity model,[7] the power flow Q_{cond} per unit area from the central plasma to the ends is

$$\begin{aligned} Q_{cond} &= 2K \frac{\partial T_e}{\partial Z} \\ &= \frac{4}{l_c} \int \frac{K}{R} dT_e \cdot \mathrm{MW/m^2} , \qquad (15) \end{aligned}$$

with $K = 9.25 \times 10^7\ T_e^{5/2}$ MW/m-keV. In this expression, l_c is the full length of the plasma column, and R is the ratio of field in the solenoid B_s to the central field B_c. We use SI units, except T_e is in keV. The power conducted along the plasma columns can be expressed by integrating Eq. (15) over T_e.

$$Q_{cond} = 3.32 \times 10^8 \frac{T_e(r)^{7/2}}{\pi l_c\ R} \cdot \mathrm{MW/m^2} . \qquad (16)$$

The theory only applies for $\lambda_e < l/2$, where λ_e is the electron-electron mean-free path,

$$\lambda_e = \frac{2 \times 10^{23} T_e^2}{n_e \ln \Lambda} \cdot \mathrm{m} . \qquad (17)$$

For $\lambda > l_c/2$, collisionless power flow due to thermal convection is the proper model.

Assuming the power loss Q_{drag} is by thermal conduction, we can equate this loss to the power input per unit area to the plasma through electron drag of injected deuterons [Eq. (9)]. Equating $Q_{cond} = Q_{drag}$, we obtain an expression for T_e:

$$T_e = 2.44 \times 10^{-10} (\hat{n}_h E_h \hat{n}_e l_h l_c R)^{1/5}\ e^{-2/5(r/a)^2} \cdot \mathrm{keV}. \qquad (18)$$

Now, integrating Eq. (16) over radius to $r_p = 2a$, we obtain

$$P_{cond} \simeq 2.39 \times 10^8 \frac{\hat{T}_e^{7/2} a^2}{l_c\ R} \cdot \mathrm{MW} , \qquad (19)$$

neglecting the power flow for $r > r_p$. In our analytic model, we used $< \sigma v >$ and $\bar{E}_h$, calculated using the multispecies FPPAC code.

In this paper we emphasize the conductivity model for primarily three reasons. First, the high-density column provides the best isolation between the hot core plasma and the refluxing gas in the end region. At the same time, a slight imbalance between the gas pressure in the two end regions provides sufficient fueling of the tritium target plasma. The second advantage of the long dense column is that the plasma temperature decreases steadily as the end regions are approached, maintaining a constant plasma pressure as n_e increases. Before impacting the end walls, we expect the ions either to recombine into gas atoms or to strike the walls with such low energy (< 10 eV)[8] that wall sputtering will not be a problem. The third, and possibly most important, advantage of the conductivity model is that the arguments for plasma stability, particularly microstability, are more certain because of the dense target plasma present in that case. The basis for stability comes both from theory and from the experience of the 2XIIB experiment. As in 2XIIB, the hot plasma is maintained in a local magnetic field minimum provided by a quadrupole magnet. The neutron-source end cells are designed to absorb the plasma power flowing out of the solenoidal Spitzer region with negligible erosion of the vacuum walls, minimum reflux of wall materials, and a minimum inventory of tritium. The plasma heat is removed by expanding the radial walls as the magnetic field lines fan to maintain the power density at the wall below 3 MW/m^2; this power flow is readily removed by conventional water-cooling techniques.

V. Neutron Source Design

For a detailed estimate of the uncollided neutron flux, we assume the source to be a linear source of finite length. The neutron flux ϕ observed at coordinates r_1, z_1 is

$$\phi = 2\pi \int_0^{r_p} n_u n_h < \sigma v > r dr \int_{-l}^{l} \frac{dz}{4\pi\,[r_1^2 + (z_1 - z)^2]} , \qquad (20)$$

where z is a source coordinate, extending from $-l$ to l. (Note: $l_h = 2l$, where l_h is total source length.) Integrating over the Gaussian distribution to obtain a source strength per unit length and then along the source length, we obtain

$$\phi = \hat{n}_u \hat{n}_h < \sigma v > \left\{ \frac{a^2}{8 r_1} \left[\tan^{-1}\left(\frac{z_1 + l}{r_1} \right) - \tan^{-1}\left(\frac{z_1 - l}{r_1} \right) \right] \right\} . \qquad (21)$$

We define the neutron wall loading Γ as the neutron power per unit area of surface at the midplane ($z_1 = 0$) and at a radius $r_1 \geq r_p$. Using Eq. (20), we obtain the following expression for Γ:

$$\Gamma = 2\pi \int_0^{r_p} n_u n_h < \sigma v > E e r dr \int_{-l}^{l} \frac{\sin\theta dz}{4\pi(r_1^2 + z^2)} , \qquad (22)$$

where $< \sigma v >$ is the reaction rate parameter obtained from Fokker-Planck runs, E is the neutron energy (14.1 MeV), e is the electronic charge, and θ is the angle between the axis and a line from the source point at z to the observation point at r_1. Integrating over the radial

Gaussian density profile and along the source length, we obtain

$$\Gamma = 1.12 \times 10^{-18} \hat{n}_w \hat{n}_h < \sigma v > \left(\frac{a^2}{2r_1}\right) \cos\theta_l \cdot \mathrm{MW/m^2}\,, \qquad (23)$$

where $\theta_l = \theta$ at $z = l$. Note that Eq. (23) is simply the value of Γ from the infinite cylindrical model, with the factor $\cos\theta_l$ correcting for the finite source length.

A. High-β Design

With $B_0 = 4$ T, a 150-keV D^+ ion has a gyroradius $\rho = 0.020$ m, making $a = 2\rho = 0.040$ m. For this case, $\sigma_{trap} \simeq 2.78 \times 10^{-20}$ m^2. With a correction factor, $1 + \delta = 1.75$, Eq. (3) gives $\hat{n}_e = 3.2 \times 10^{21}$ m^{-3}. The hot-ion density is determined by the β limit, which for this base case is taken as $\hat{\beta} = 1$ consistent with 2XIIB operation. Thus, neglecting other small contributions to β,

$$\hat{n}_h = \frac{\hat{\beta} B^2}{4 \times 10^{-22} E_h} = 8 \times 10^{20}\ \mathrm{m^{-3}}\,, \qquad (24)$$

where $E_h = 50$ keV as estimated from Fokker-Planck calculations. For the hot plasma length, we selected a value of $l_h = 0.15$ m. This is a compromise to yield a moderate-sized test volume with good performance at a reasonable power level and at demonstrated neutral-beam densities.

As seen from Eq. (18), T_e can be modestly increased by increasing the magnitude of the field and the length l_c of the power transport region. We consider the maximum practical field strength B_s to be 12 T, consistent with demonstrated magnet performance.[9] We chose $l_c = 10$ m as a standard length for all cases, since the gain beyond $l_c = 10$ m is small. The power of the injected beam is equal to that lost by conduction and is given by Eq. (19). Parameters for the high-β design are listed in Table II.

Table II: Operating Point Parameters.

	High β 0.15 m	Low β 0.3 m	Low β 0.075 m
D^0 beam energy (keV)	150	150	150
D^0 beam power (MW)	60	50	13
Γ (MW/m^2)	7.2	11.6	4.9
Fusion power (MW)	1.0	1.1	0.17
Plasma (peak) β	1.0	0.25	0.16
$\hat{n}_h$ ($r = 0$) (m^{-3})	8×10^{20}	8×10^{20}	5×10^{20}
$\hat{n}_e$ ($r = 0$) (m^{-3})	3.2×10^{21}	6.3×10^{21}	6.3×10^{21}
T_e ($r = 0$) (keV)	0.22	0.21	0.14
E_h (keV)	50	51	46
l_h (m)	0.15	0.30	0.075
a (m)	0.04	0.02	0.02
$r_p = 2a$ (m)	0.08	0.04	0.04
ρ_i (m)	0.02	0.01	0.01
l_c (m)	10	10	10
B_0 (T)	4	8	8
B_s (T)	12	12	12
Magnet power (MW)	6.8	0	0

B. Low-β Design

At sufficiently low β, MHD stability can be provided in axisymmetric linear systems by rf ponderomotive forces or by providing sufficient perpendicular plasma pressure in regions of positive curvature.[10] Eliminating the quadrupole magnet greatly simplifies magnet design, improves access to the plasma, and reduces operating cost by reducing power consumption. Although the data base for these approaches to MHD stability is not as extensive as that for quadrupole stabilization, it is sufficient to warrant consideration of these systems as neutron sources. In the design discussed below, the exiting magnetic field lines have strong positive curvature similar to that in the Gas Dynamic Trap[10] experiment, where MHD stability is provided by the pressure of the end-loss plasma. In the axisymmetric design, β is reduced without sacrificing plasma density by increasing the magnetic field B_c to 8 T. At 8 T, the plasma radius r_p is reduced from 0.08 m in the high-β design to 0.04 m. With the reduced plasma size the density can be increased to $\hat{n}_e = 6.3 \times 10^{21}$ m^{-3} with adequate beam penetration. At 8 T using 50 MW of beam power, Γ at the plasma surface is 160% that of the 4-T, 60-MW design. The 8-T, 50-MW design also provides a factor of two gain in sample volume and a reduction by a factor of four in β compared to the 4-T, 60-MW design.

Table III gives plasma size and parameters for one high-β design, three low-β designs, and an earlier accelerator-based D-Li neutron source.[11]

VI. Summary

In this paper we have described the conceptual design of a fusion D-T neutron source based on plasma physics and technologies developed in the international effort to develop fusion power. Freedom from the requirement of net power production has permitted the design of a system that is relatively small and low-cost, has low physics risk, and requires little development. Because the D-T reaction is restricted to a small volume, the volume of activated material and tritium consumption are small. The total neutron production rate is approximately proportional to injected beam power and, because the beam system is the largest cost item, the construction cost increases nearly linearly with the total neutron production.

Acknowledgments. The authors thank T.K. Fowler, D.E. Baldwin, H.L. Berk, and T.C. Simonen for many helpful discussions of the plasma physics design. A.A. Mirin of the National Magnetic Fusion Energy Computer Center provided assistance on the FPPAC Fokker-Planck codes. This work was performed under the auspices of the U.S. Department of Energy by Lawrence Livermore National Laboratory under Contract W-7405-Eng-48.

Table III: Neutron Source Parameters.

Neutron source beam energy (keV)	Central field (T)	Plasma size, $L \times r_p$ (m)	β	Beam power (MW)	Neutron power (plasma edge) (MW/m^2)	Total source (n/s)	Volume, $\phi >$ 10^{14} n/cm^2·s (liters)
150	4	0.15 × 0.16	1.0	60	7.2	3.6×10^{17}	8.7
150	8	0.30 × 0.08	0.25	50	11.6	4.1×10^{17}	17
150	8	0.15 × 0.08	0.16	21	6.5	1.22×10^{17}	2.0
150	8	0.075 × 0.08	0.16	13	4.9	0.6×10^{17}	0.48
FMIT* (35 MeV D^+ beam, Li target)				7		0.3×10^{17}	0.48

*FMIT = Fusion Materials Irradiation Test Facility

References

[1] *Technical Planning Activity, Final Report*, chapter 5, Argonne National Laboratory, Argonne, IL, ANL/FPP-87-1 (1987).

[2] W.C. Turner et al., *Nucl. Fusion*, **19**, 1011 (1979).

[3] R.F. Post, T.K. Fowler, J. Killeen, and A.A. Mirin, *Phys. Rev. Lett.*, **31**, 280 (1973).

[4] C.D. Boley, R.K. Janev, and D.E. Post, *Phys. Rev. Lett.*, **52**, 534 (1984).

[5] M.G. McCoy, A.A. Mirin, and J. Killeen, *Comput. Phys. Commun.*, **24**, 37 (1981).

[6] B.G. Logan, I.G. Brown, and M.A. Lieberman, *Phys. Fluids*, **17**, 1302 (1974).

[7] L. Spitzer, Jr., *Physics of Fully Ionized Gases* (Interscience Publishers, New York, 1956), 86.

[8] W.L. Hsu, M. Yamada, and P.J. Barrett, *Phys. Rev. Lett.*, **49**, 1001 (1982).

[9] F.H. Coensgen et al., "MFTF-B Acceptance Tests and Operation," *Proc. 11th Int. Conf. Plasma Phys. Cont. Nucl. Fusion Research* (Kyoto, Japan, November 13–20, 1986).

[10] P.A. Bagryanskii et al., in *Proc. 11th Int. Conf. Plasma Phys. Cont. Fusion Research*, Kyoto, 1986 (International Atomic Energy Agency, Vienna, 1987).

[11] R.J. Burke et al., "Super-FMIT, an Accelerator-Based Neutron Source for Fusion Components Irradiation Testing," *Nucl. Instr. and Meth.*, **B10/11**, 483 (1985).